Available online at www.sciencedirect.com
SCIENCE DIRECT®
Journal of Power Sources 115 (2003) 125–130
JOURNAL OF POWER SOURCES
www.elsevier.com/locate/jpowsour

Short communication

Electrochemical characteristics of orthorhombic $LiMnO_2$ with different degrees of stacking faults

Jung-Min Kim, Hoon-Taek Chung*

Department of Ceramic Engineering, Dongshin University, Naju, Chonnam, Republic of Korea

Received 19 February 2002; accepted 29 November 2002

Abstract

Orthorhombic $LiMnO_2$ (*o*-$LiMnO_2$) is known to have stacking faults (local regions of monoclinic ordering) that are caused by structure disorder between Li and Mn sites. Previous research has indicated that this structural disorder, correlated with the full width at half maximum (FWHM) of the (1 1 0) X-ray diffraction (XRD) peak, might affect the electrochemical properties of *o*-$LiMnO_2$. In this study, *o*-$LiMnO_2$ powders are prepared by an emulsion drying method. Different degrees of stacking faults are induced by varying the heating rate. From electrochemical and ex situ XRD experiments, it is found that a sample with a high number of stacking faults undergoes easier phase transformation from the orthorhombic to the spinel structure on cycling. This form of *o*-$LiMnO_2$ displays no capacity fading in the 4 V (versus Li/Li^+) region, but suffers severe capacity fading in the 3-V region. By contrast, a sample with a low number of stacking faults experiences no capacity fading in either the 3- or 4-V regions and has good cycleability.

Keywords: Capability; Orthorhombic; $LiMnO_2$; Emulsion drying; Stacking faults; Li-ion battery

1. Introduction

The Li–M–O intercalation system (M: Co, Ni, Mn) has been investigated intensively as positive-electrode (cathode) material for lithium secondary batteries. Among the various compounds in the system, $LiMnO_2$ has several advantages over $LiCoO_2$ or $LiNiO_2$, namely: less toxicity, lower cost, and ready availability of Mn. $LiMnO_2$ can have an orthorhombic (*Pmnm*) or a monoclinic (*C/2m*) structure, i.e. the compound is polymorphous. The former structure was first assigned by Johnston and Keikes [1], while the latter was obtained through ion-exchange from $NaMnO_2$ by Armstrong and Bruce [2]. The two different structures both transform to a spinel-like structure on cycling; *o*-$LiMnO_2$ transforms when it is cycled between 3 and 4 V (note, all potentials are reported versus Li/Li^+) [3–6]. X-ray diffraction (XRD) studies have verified that this irreversible transformation into a spinel-like structure on initial cycling is consistent with the appearance of two plateaux at 3 and 4 V, respectively [7,8]. Vitins and West [9] confirmed, by XRD analysis, that monoclinic $LiMnO_2$ (*m*-$LiMnO_2$) also converts from its original structure to a spinel-like structure, and reported the development of plateaux at 3 and 4 V during cycling.

Groguennec et al. [4] showed, by ex situ XRD studies, that small crystallites/crystals of 1–10 μm size are more easily transformed to a spinel-like structure. They also proposed that *o*-$LiMnO_2$ has stacking faults (local regions of monoclinic ordering) that are caused by structural disorder between Li and Mn sites, and that these stacking faults, which induce widening of the (1 1 0) XRD peaks, can improve the electrochemical performance of *o*-$LiMnO_2$ [10,11]. Recently, however, Jang et al. [12] and Myung et al. [13] found that well-ordered *o*-$LiMnO_2$ with only about 1% stacking faults displays good cycleability. Thus, the effect of stacking faults on the electrochemical performance of *o*-$LiMnO_2$ is still not fully understood.

The three polymorphs—*o*-$LiMnO_2$, *m*-$LiMnO_2$ and spinel-$LiMn_2O_4$—are based on a cubic close-packed oxygen sub-lattice and differ mainly in terms of cation ordering. When lithium ions are electrochemically removed from *o*-$LiMnO_2$ and *m*-$LiMnO_2$, a spinel-like structure can be produced by moving 50% of the Mn ions from the 2a octahedral sites in *o*-$LiMnO_2$ [6,7] and 25% of the Mn ions from 2a octahedral sites in *m*-$LiMnO_2$ to 16d octahedral sites in the spinel [14]. This suggests *m*-$LiMnO_2$ may be easier to transform into the spinel-like structure than

* Corresponding author. Fax: +82-61-330-2909.
E-mail address: htchung@white.dongshinu.ac.kr (H.-T. Chung).

0378-7753/03/$ – see front matter
doi:10.1016/S0378-7753(02)00709-7

o-$LiMnO_2$. If m-$LiMnO_2$ exists as stacking faults at local regions within o-$LiMnO_2$, then it might influence the phase transformation of o-$LiMnO_2$ to the spinel-like structure. In this study, therefore, different degrees of stacking faults in o-$LiMnO_2$ samples of similar crystal size (about 1 μm) are obtained by heat treatment, and an examination is made of the effect of these stacking faults on the electrochemical characteristics of o-$LiMnO_2$ on charge−discharge cycling.

2. Experimental

The $LiMnO_2$ precursor was prepared from a mixture of $LiNO_3$ and $Mn(NO_3)_2{\cdot}6H_2O$ (1:1 mol ratio) by means of an emulsion drying method. The detailed powder preparation route has been described previously [15]. The precursor was calcined at 400 °C for 2 h in air. The resulting powder was heated to 850 °C and then held at this temperature for 12 h in an argon atmosphere. It was found that the degree of stacking faults in o-$LiMnO_2$ can be controlled by the heating rate. Therefore, o-$LiMnO_2$ samples with different degrees of stacking faults were prepared by heating calcined powders for 8 h (1.7 °C min^{-1}), 11 h (1.3 °C min^{-1}) and 14 h (1 °C min^{-1}) up to 850 °C. These samples are termed H8, H11 and H14, respectively, and were characterized by XRD diffraction and determination of the full width at half maximum (FWHM) of the (1 1 0) peak.

For electrochemical testing, a positive-electrode (cathode) slurry was fabricated by mixing the prepared o-$LiMnO_2$ powder, acetylene black and polyvinylidene fluoride (PVDF) in a weight ratio of 75:15:10 in N-methly-2-pyrolidinone (NMP). The slurry was pasted on nickel exmet (1 cm^2) and dried at 120 °C for 2 days under vacuum. Cells were assembled in an argon-filled glove box and used the cathode as the working electrode, lithium ribbon of 0.35 mm thickness as the counter electrode, and 1 M $LiClO_4$ in a propylene carbonate (PC) as the electrolyte. Electrochemical tests were performed on the cells between 2.0 and 4.3 V at a constant current density of 20 mA g^{-1} at 30 °C. To confirm the transformation of o-$LiMnO_2$ into the spinel-like structure, ex situ X-ray diffraction measurements were taken on samples after the 1st, 3rd and 5th discharges, as well as after the 10th charge. In each case, the sample was held for 3 h at the respective end of discharge or charge voltage.

3. Results and discussion

The XRD data of powders calcined at 850 °C for 12 h in an argon atmosphere are shown in Fig. 1. The inset shows that there is no (4 4 0) spinel peak around 64°. All powders have o-$LiMnO_2$ as a dominant phase (Miller indices) and a small amount of Mn_3O_4 and MnO. Although all the XRD peaks of the o-$LiMnO_2$ phases are nearly same, the (1 1 0) peak which correlates with the stacking faults in o-$LiMnO_2$ gradually becomes sharp and strong with decreasing heating rate. The widening of this peak occurs when the degree of stacking faults in o-$LiMnO_2$ increases [11]. The FWHM of the (1 1 0) peak versus heating rate for each sample is given in Fig. 2; the peak value for samples H8, H11 and H14 is 0.5786, 0.4544 and 0.2357°, respectively. These values indicate that the degree of stacking faults decreases with decreasing heating rate, i.e. H14 has an orthorhombic structure with less stacking faults than either H8 or H11. Therefore, it is concluded that the degree of stacking faults can be controlled by the heating rate because all the powders were prepared under the same conditions (i.e. calcination temperature, holding time and atmosphere) except for the heating rate.

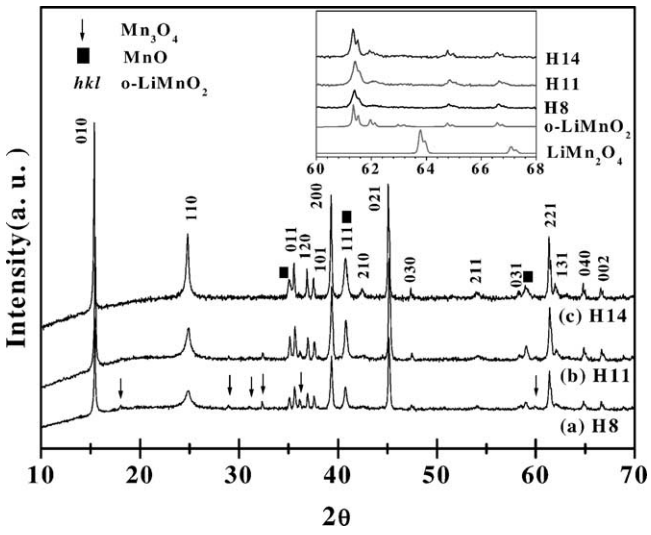

Fig. 1. XRD patterns of (a) H8, (b) H11 and (c) H14 calcined at 850 °C for 12 h in Ar. Miller indexes indicate o-$LiMnO_2$ (*Pmnm*). In inset, XRD patterns for o-$LiMnO_2$ and spinel-$LiMn_2O_4$ are simulated from JCPDS 35-0749 and 35-0782, respectively.

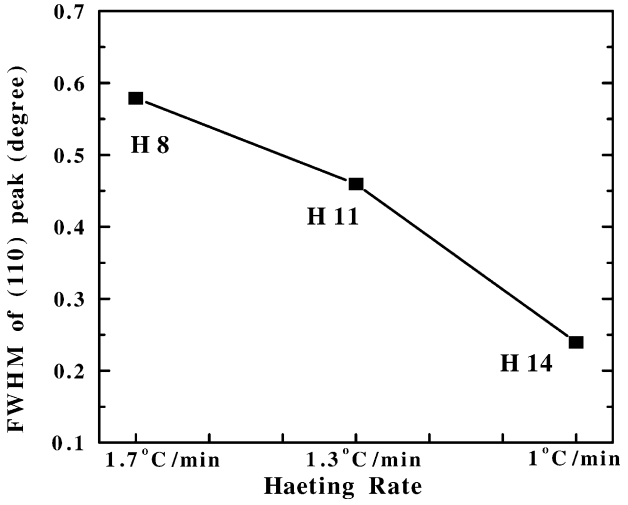

Fig. 2. Full width at half maximum of (1 1 0) peak vs. heating rate.

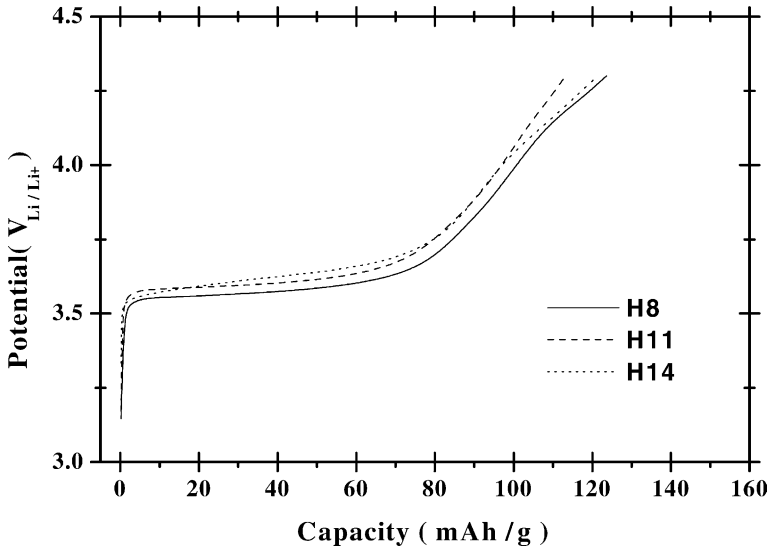

Fig. 3. Electron micrographs of (a) H8, (b) H11 and (c) H14 samples calcined at 850 °C for 12 h.

It is well known that the electrochemical properties of *o*-$LiMnO_2$ are affected by its crystal size because the diffusion of Li ions in the pristine state is too slow. Thus, the first charge capacity correlates with the crystal size. For example, Groguennec et al. [4] showed that about 0.9, 0.6 and 0.3 Li ions were extracted from crystals of size 0.3, 1 and 10 μm, respectively. The first charge capacities of samples H8, H11 and H14 are 123, 113 and 121 mA h g^{-1}, respectively (Fig. 3). These results indicated that the samples have similar crystal size. Scanning electron micrographs confirm that this crystal size is 1 μm (see Fig. 4). Therefore, in the experiments performed in this study, the electrochemical behaviour of the cathode materials is affected not by crystal size but by structural disorder.

The differential discharge capacity plots for the cycles 1, 3, 5 and 10 of samples H8, H11 and H14 are presented in Fig. 5. Both the 4- and 3-V reduction peaks—which correlate with lithium insertion in tetrahedral and octahedral sites in spinel structure, respectively—increase in all samples. This behaviour indicates that phase transformation occurs in all samples during cycling [12]. There are, however, some differences. The sample with a high number of stacking faults, i.e. H8, shows dramatic growth and peak splitting of the peak at 4 V on the third and fifth cycles, as shown in Fig. 5(a). By contrast, H14 with a low number of stacking faults exhibits slow development of the 4-V reduction peak, and peak splitting only occurs on the 10th cycle. These observations indicate that the transformation from an orthorhombic into a spinel-like structure becomes faster with increase in the number of stacking faults.

The ex situ XRD results for samples after the first, third and fifth discharges are presented in Fig. 6. After the first discharge, a distinct (1 1 1) spinel peak emerges in the higher stacking faulted samples H8 and H11, but only a weak broad (1 1 1) spinel peak is observed in the lower stacking faulted sample H14. In the case of H8 and H11, the

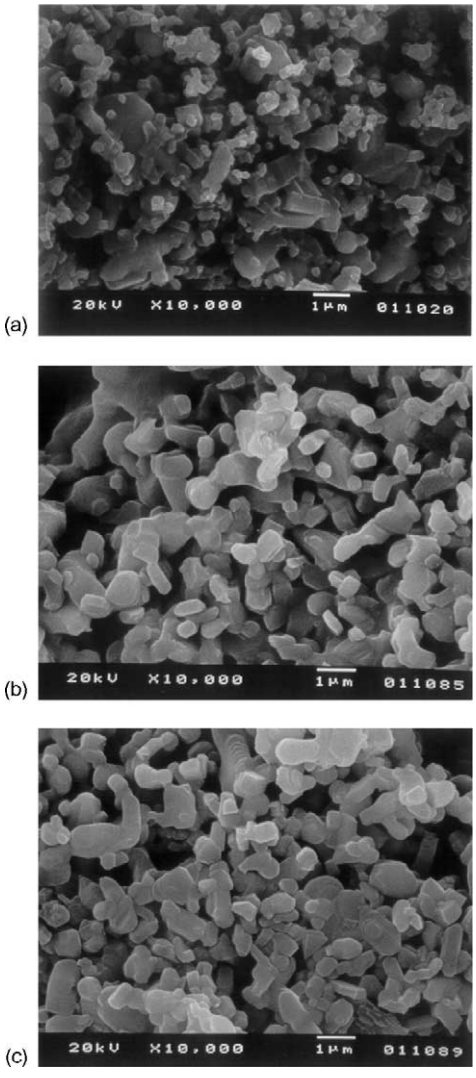

Fig. 4. First charge capacities of samples up to 4.3 V, current density 20 mA g^{-1}.

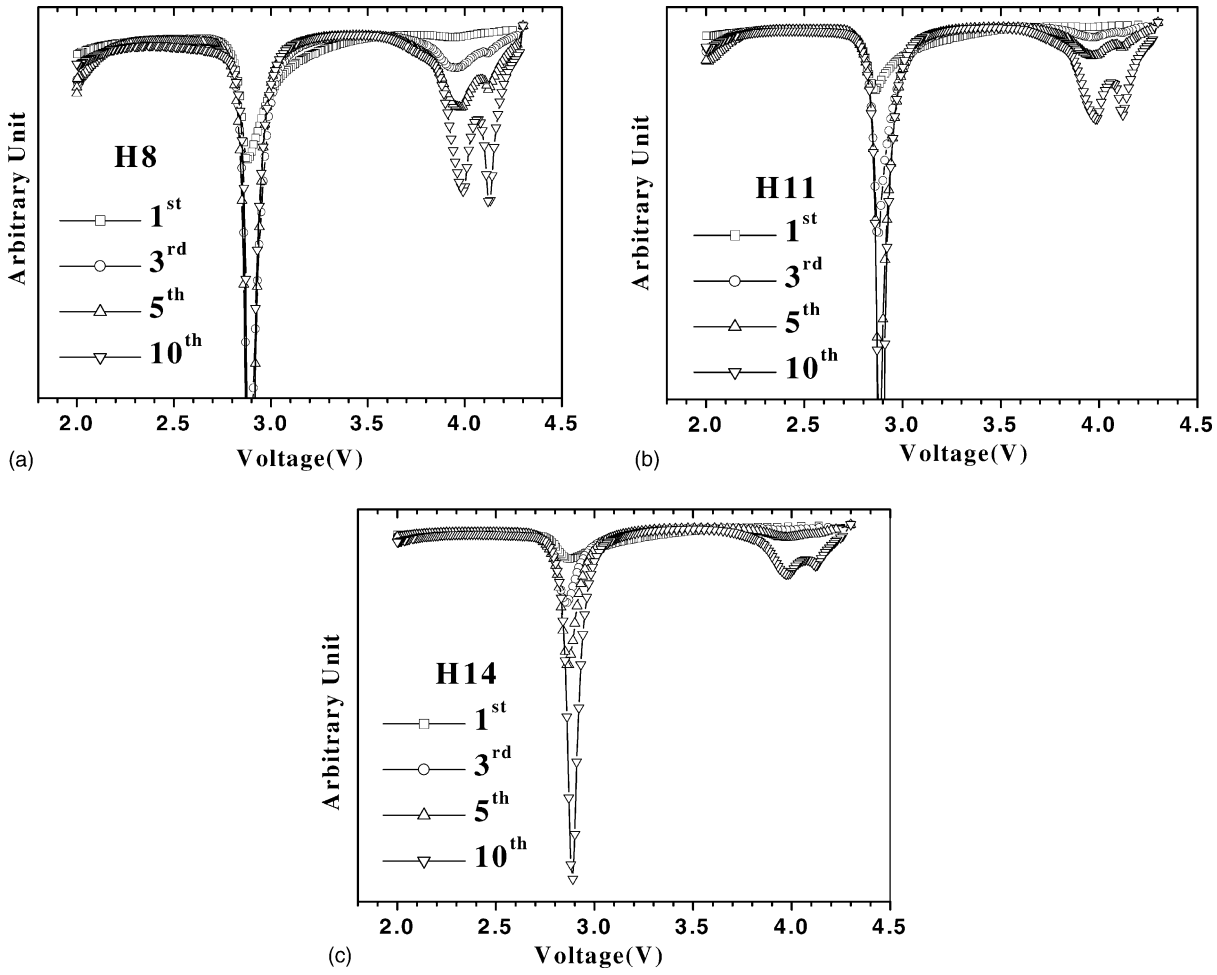

Fig. 5. Evolution of differential discharge capacity plots on cycling for (a) H8, (b) H11 and (c) H14 cycled between 2.0 and 4.3 V at 30 °C (current density, 20 mA g^{-1}).

intensity of the (1 1 1) spinel peak becomes stronger than that of the (0 1 0) *o*-$LiMnO_2$ peak with cycling, whereas H14 shows that the intensity of the (0 1 0) *o*-$LiMnO_2$ peak is still higher than that of the (1 1 1) spinel peak after the fifth discharge. Given that the crystal size of the samples is similar, viz. 1–2 μm, these findings differ from those of Groguennec et al. [4]. This suggests that the phase transformation is dependent on crystal/crystallite size, and that a large size results in unreacted *o*-$LiMnO_2$ after 50 cycles. The X-ray data for samples after the 10th charge at 4.3 V are given in Fig. 7. All the orthorhombic phases have transformed into a spinel-like phase which is indexed as a cubic spinel. Thus, electrochemical and corresponding X-ray data are in agreement in that the transformation from an orthorhombic to a spinel-like structure becomes easier (or faster) with an increasing number of stacking faults. Therefore, it is possible that the phase transformation of samples is affected by structural disorder, i.e. by stacking faults, when the crystal size is similar.

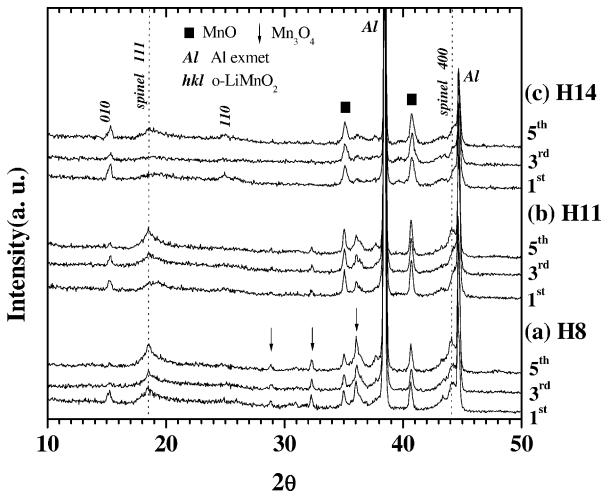

Fig. 6. Ex situ X-ray data for first, third and fifth discharged samples of (a) H8, (b) H11 and (c) H14 maintained at 2.0 V end-of-discharge for 3 h.

The discharge capacities of samples on cycling between 2.0 and 4.3 V at 20 mA g^{-1} and 30 °C are given in Fig. 8(a). Sample H14 shows good performance up to 100 cycles, whereas H8 and H11 experience capacity fading. The capacity is presented in terms of the 3- and 4-V regions, as shown in Fig. 8(b) and (c), respectively. H14 retains its

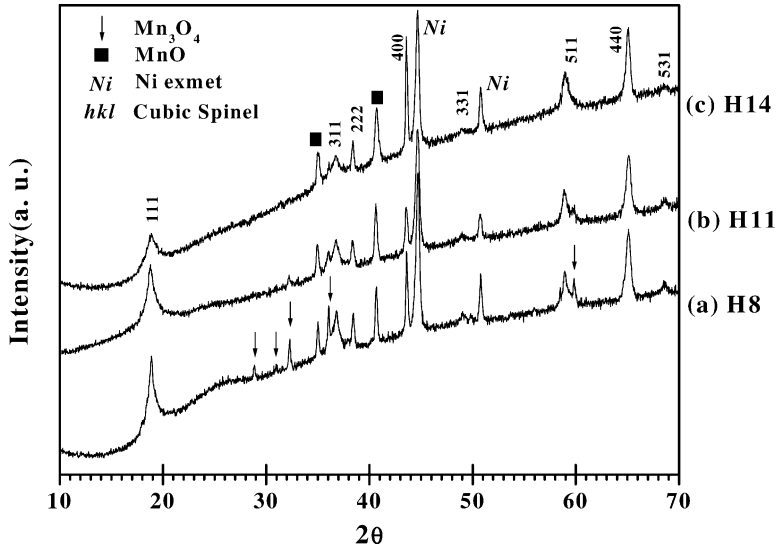

Fig. 7. Ex situ X-ray data for 10th charged sample of (a) H8, (b) H11 and (c) H14 maintained at 4.3 V end-of-charge for 3 h.

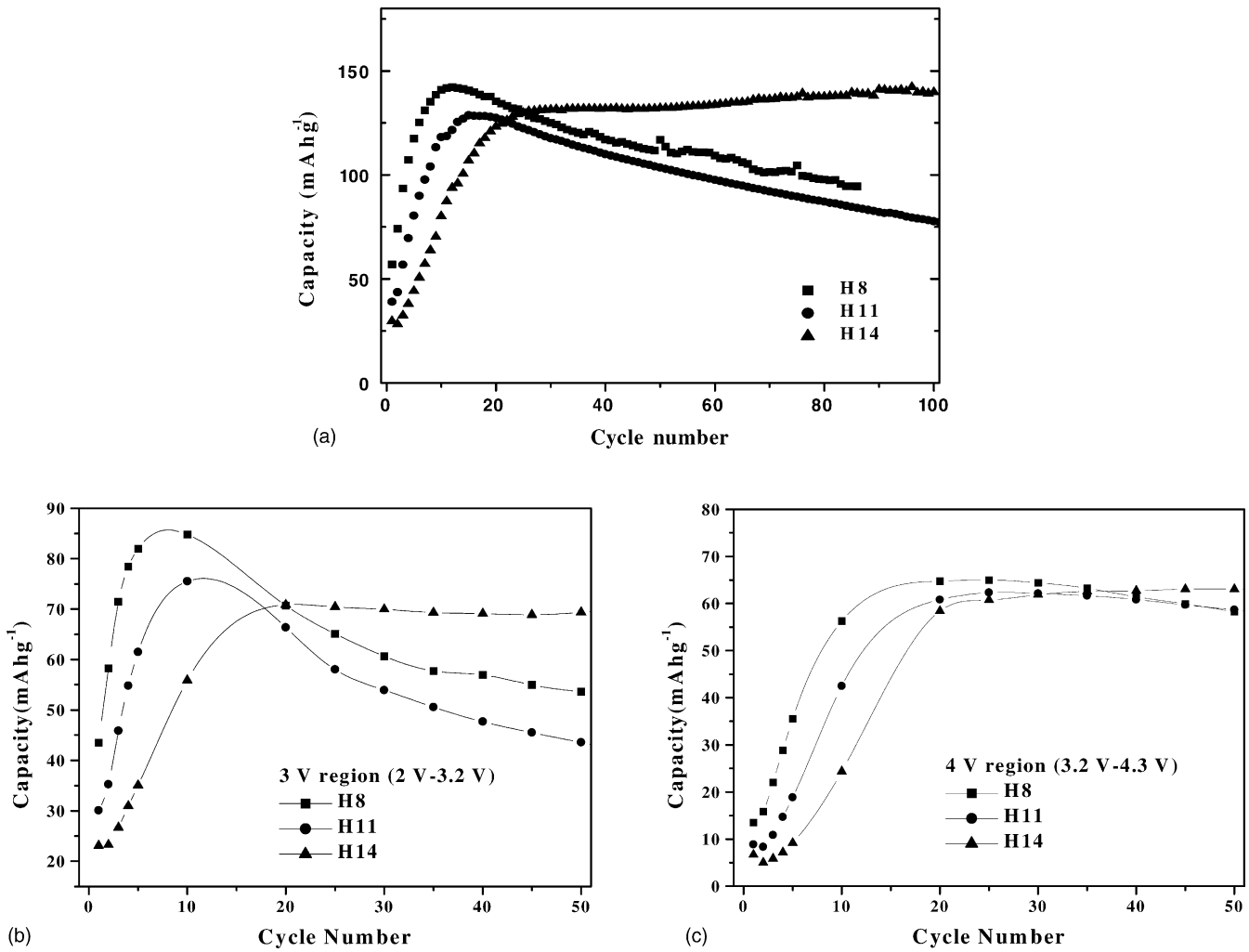

Fig. 8. Discharge capacities of samples as a function of cycle number (a) 3- and 4-V regions, (b) 3-V region and (c) 4-V region.

capacity in both regions, whereas H8 and H11 retain their capacity in the 4-V region, but display severe capacity fading in the 3-V region. Wang et al. [16] have suggested that the anti-phase domains in the spinel structure generated from $LiMnO_2$ by cycling are able to accommodate the Jahn–Teller induced strain. In the experiments reported here, the fact that all powders transformed into the spinel-like structure after 10 cycles, but exhibit different characteristics in the 3-V region with further cycling is still to be explained. On the other hand, the (1 1 1) spinel peak becomes broader with decrease in the degree of stacking faults, as shown in Fig. 6. Therefore, it can be assumed that the peak broadening in the XRD spectrum is due to domains in the structure, and this is one of the reasons why H14, which has such domains, shows good cycleability.

4. Conclusions

o-$LiMnO_2$ powders with different degrees of stacking faults, but with similar crystal size, are prepared by controlling the heating rate. It is found that the transformation from the orthorhombic structure to the spinel-like structure becomes easier (or faster) with increase in the degree of stacking faults, as expected from structural considerations. *o*-$LiMnO_2$ with a low number of stacking faults displays better cycleability than a high stacking faulted version when cycled between 2.0 and 4.3 V. Studies are in progress to understand this behaviour.

Acknowledgements

This work was supported by grant no. R05-2001-000-00808-0 from the Basic Research Program of the Korea Science and Engineering Foundation.

References

[1] W.D. Johnston, R.R. Keikes, J. Am. Chem. Soc. 78 (1956) 3255.
[2] R. Armstrong, P.G. Bruce, Nature (1996) 381.
[3] I.J. Davidson, R.S. McMillan, J.J. Murray, J.E. Greedan, J. Power Sources 54 (1995) 232.
[4] L. Groguennec, P. Deniard, R. Brec, J. Electrochem. Soc. 144 (1997) 3323.
[5] M.M. Thackeray, J. Electrochem. Soc. 142 (1995) 2558.
[6] W. Tang, H. Kanoh, K. Ooi, J. Solid State Chem. 142 (1999) 19.
[7] R.J. Gummow, D.C. Liles, M.M. Thackeray, Mater. Res. Bull. 28 (1993) 1249.
[8] I.M. Kotschau, J.R. Dahn, J. Electrochem. Soc. 145 (1998) 2672.
[9] G. Vitins, K. West, J. Electrochem. Soc. 144 (1997) 2587.
[10] L. Groguennec, P. Deniard, R. Brec, A. Lecerf, J. Mater. Chem. 7 (1997) 511.
[11] L. Groguennec, P. Deniard, R. Brec, A. Lecerf, J. Mater. Chem. 5 (1995) 1919.
[12] Y.I. Jang, B. Huang, H. Wang, D.R. Sadoway, Y.M. Chiang, J. Electrochem. Soc. 146 (1999) 3217.
[13] S.T. Myung, S.H. Komaba, N. Kumagai, Chem. Lett. (2001) 574.
[14] J. Reed, G. Ceder, A. Van Der Ven, Electrochem. Solid-State Lett. 4 (2001) 78.
[15] S.-T. Myung, H.-T. Chung, J. Power Sources 84 (1999) 32.
[16] H. Wang, Y.-I. Jang, Y.-M. Chiang, Electrochem. Solid-State Lett. 2 (1999) 490.